A method for accelerated ageing tests of photovoltaic inverters considering the application's mission profiles

Mouhannad-G. DBEISS[1, 2], Yvan AVENAS[2], Henri ZARA[1], Laurent DUPONT[3]
[1]FRENCH ALTERNATIVE ENERGIES AND ATOMIC ENERGY COMMISION-NATIONAL SOLAR ENERGY INSTITUTE (CEA-INES)
[2]UNIV. GRENOBLE ALPES, CNRS, G2Elab
[3]SATIE IFSTTAR
[1]Le Bourget du Lac, France ; [2]Grenoble, France ; [3]Versailles, France
T. +33 (0)4 79 79 21 44 | F. +33 (0)4 79 68 80 49
Mouhannad.Dbeiss@cea.fr | yvan.avenas@g2elab.grenoble-inp.fr

Acknowledgments

This project has received support from the State Program Investment for the Future" bearing the reference. (ANR-10-ITE-0003)

Keywords

«Mission profile» «Renewable energy systems» « (VSC) Voltage Source Inverters» «Reliability» «Thermal cycling»

Abstract

This paper presents a new method for the accelerated ageing tests of photovoltaic inverters, created by analyzing the mission profiles of the current and ambient temperature extracted over several years from multiple photovoltaic plants located in France. It is proposed to create a particular ageing profile which takes into account not only the different constraints of the application of the photovoltaic inverters (high-frequency switching and sinusoidal-shaped current), but also reproduces a typical profile of the output current of photovoltaic inverters. Similarly, thermal cycling is applied simultaneously by varying the ambient temperature as in the real application, and by applying current injections with relatively long durations, which will lead to a rise in the temperatures of the DBC substrates and the coolers. This method should show better representation of the thermal behavior of DC/AC inverters used in photovoltaic applications, and is expected to give results that are more representative than traditional power cycling, and thus reducing the favoring of certain failure modes to the detriment of others.

1. Introduction

In photovoltaic systems, the DC/AC inverter has the highest failure rate, and the anticipation of its breakdowns is still difficult [1]. Thus it is crucial to accelerate the ageing of the devices included in this converter in order to study its main failure modes. In this context, accelerated ageing of power modules is carried out under aggravated conditions of current (Power Cycling) or temperature (Thermal Cycling) to speed up the normal ageing processes. It is used to help determining, in a laboratory, the long-term effects of expected levels of stress within a shorter period of time. Unfortunately, by applying the accelerated ageing, mechanisms of failures that do not occur in the real application could be observed, and inversely other mechanisms that usually occur could be not created [2].

This paper presents a new method for the accelerated ageing of photovoltaic inverters, considering the mission profiles of the current and ambient temperature, extracted from photovoltaic plants for several years. These profiles are used to study the dynamics of the photovoltaic current, and are introduced into a numerical model to estimate the variations of the junction temperature of the semi-conductor power devices used in the inverter, using the "Rainflow" counting method. The result of this study is a new accelerated ageing method inducing simultaneously active and passive cycling under switching nominal conditions and pulse width modulation (PWM) operating mode. This method is expected to be more representative of the natural ageing process of the power modules in inverters than the traditional accelerated ageing processes.

The thermal cycling consists of cycling the devices between two extreme temperatures, and inducing usually big variations in the module temperature. The power cycling consists of applying a series of current pulses, usually resulting to large variations of the junction temperature of semiconductor devices [3] [4]. The power cycling using the opposition method consists of switching the power modules, putted in a single-phase PWM inverter and under nominal conditions. It is a power cycling method with more realistic electrical stresses on the power devices compared with the classical power cycling. The devices are fed with a regulated sinusoidal current with an adjustable frequency. For power semiconductor devices, the operating conditions are very close to those existing in a drive inverter [5] [6].

The accelerated ageing methods mentioned above are widely used but do not necessarily represent always the real application [7]. In this paper, a new method is proposed, and mission profiles of the current and ambient temperature, extracted from photovoltaic power plants for several years are used to analyze their dynamics, and create an accelerated ageing profile respecting the characteristics of the photovoltaic application. The complete approach of the study is resumed in Fig. 1.

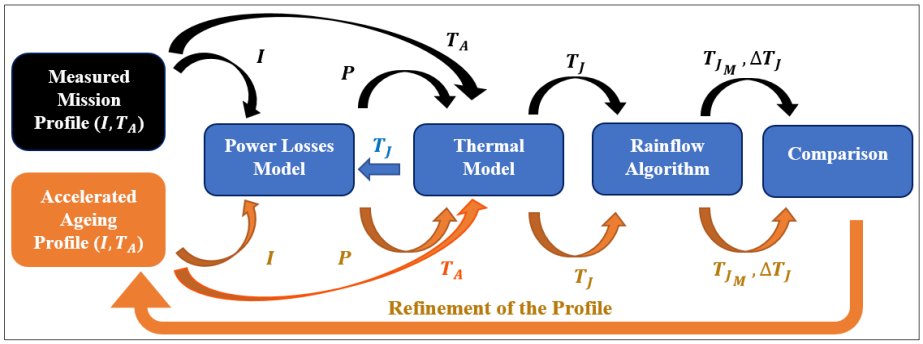

Fig. 1: Current and ambient temperature mission profiles over a clear sky day.

The current mission profile, that represents the RMS output current of the DC/AC inverter, is introduced into a power losses estimation model that gives at its output the corresponding power losses. These losses are then introduced, along the ambient temperature mission profile into a thermal model to estimate the junction temperature of the semiconductor devices. These two models are developed with Matlab and are coupled in order to take into account the variations of the losses depending on the temperature of semiconductor devices [3]. Temperature, estimated as a function of time, is then injected into a cycle counting algorithm named "Rainflow" that allows to obtain, for a given temperature profile, the number of occurrences for each value of temperature swing ΔT_J. In the approach shown in Fig. 1, I is the RMS current profile at the output of the inverter over a fundamental period (here 20 ms), P the losses profile for a given semiconductor component, T_J the junction temperature profile, ΔT_J the temperature swings, T_{J_M} the mean temperature of each temperature swing and T_A the ambient temperature.

2. Building the accelerated ageing profile

2.1. Analysis of photovoltaic data

The analysis of the mission profiles will be presented in this section. In the case of the photovoltaic application, the RMS current at the output of the inverters is proportional to the solar irradiance, which in its turn can be described with mathematical equations arising from the rotation of the earth around itself (variation over a day) and around the sun (variation over a year). The profiles of the current and ambient temperature, extracted over several years from photovoltaic plants located in France can present clear sky days (Fig. 2), and cloudy days (Fig. 3).The variations of the current presented in Fig. 3 cause numerous and sudden variations of the junction temperature of the power semiconductors during the day. The latter is one of the most important factors in the ageing of photovoltaic inverters [8] [9]. After the analysis of the current profiles, several characteristics can be noticed and will be detailed in the next paragraphs.

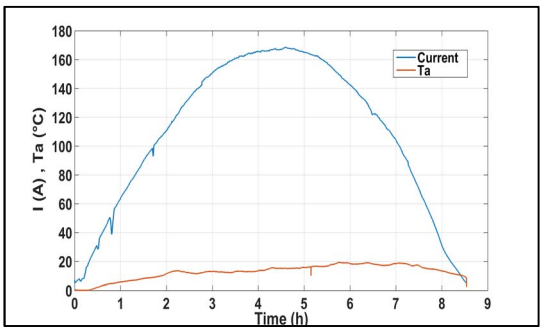

Fig. 2: I and T_A mission profiles over a clear sky day.

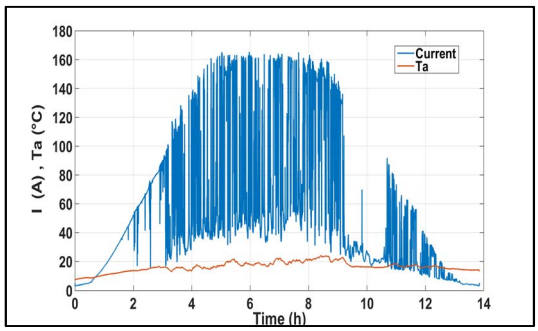

Fig. 3: I and T_A mission profiles over a cloudy day.

2.1.1. The shape of the current

The shape of the generated current, that represents the RMS output current of the DC/AC inverter, during the sunshine can be described by a complex mathematical equation that can be presented by the general form $\alpha \cdot \sin(t) \cdot \cos(t)$, where t is a term including time and α a variable term designating several parameters, such as the geographical area and the orientation of the photovoltaic panels and many other parameters [10]. The sunshine hours differ from a season to another and from a geographical zone to another, and during the night there is no current produced by the photovoltaic panels.

2.1.2. The diffuse radiation

The minimum value that can be reached by the current during a day is proportional to the diffuse radiation. Diffuse radiation results from diffraction of sunlight by the clouds and its scattering by the various molecules and particles suspended in the atmosphere, and its refraction by the ground. This is therefore a radiation which does not follow a direction defined by the sun in the direction of the observation point on the surface of the Earth. This irradiation at a given moment is close to 10% of the total irradiation. Thus the current produced during the passage of clouds at a given moment is close to 10% of the total current that the photovoltaic panels produced directly before the passage of the clouds [11].

2.1.3. The slope of the current variations

As shown in Fig. 3, the variation speed of the RMS current value can be very fast due to the cloudy passageway. It depends on the wind speed and also on the size of the photovoltaic plant linked to the inverter. With the available data, the maximum slope of these sudden variations is estimated to be $0.15 \times I_{MAX}$ (A/s) where I_{MAX} is the maximum RMS current reached during one year. This specific value of the photovoltaic application is obtained through statistical studies carried out on current measurements at the output of photovoltaic power plants in France, so it can varies from a geographical area to another. However, considering this slope during the accelerated ageing of DC/AC inverters is very important, because the variations applied in a traditional accelerated ageing are abrupt

and accelerate the damaging of the module (potentially in a not-representative way of the photovoltaic application).

2.1.4. Seasons

All the seasons show the same characteristics but, in the south of France, spring is the most constraining one, because it brings together high number of sunshine hours, high radiation/current levels and a maximum number of big variations of the current due to the cloudy periods.

2.1.5. The ambient temperature

The ambient temperature has a "sinusoidal" shape during the day (Fig. 2 and Fig. 3), and its limits of variations depend on the geographical area, but it generally varies along the year as presented in Fig. 4. As it can be noticed, the variations of the temperature during the day can be higher than 20°C.

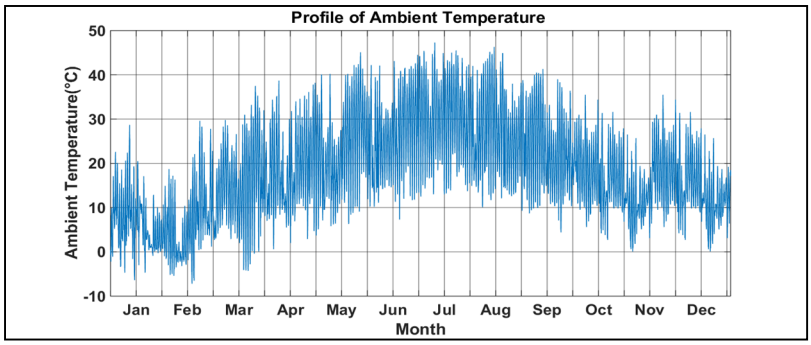

Fig. 4: The ambient temperature profile over year 2015.

2.1.6. Delays between the current variations

To build a profile that allows to accelerate the ageing of the power modules of the DC/AC photovoltaic inverter, it was chosen to neglect the small variations. Thus in this study, only the delays between the variations of the current higher than ΔI_{min} , that introduce $\Delta T_J \geq 30\,K$ were arbitrary taken into consideration. The value of ΔI_{min} can be determined using the thermal model described in section 3.2. The histogram presented in Fig. 5 shows the percentage of the occurrences of the delays between these big variations of the current (T_{on} and T_{off}), in other words the delays between 2 consecutive passages of clouds inducing high temperature swings. More than 50% of these delays are higher than $120\,s$, so they are all presented with one bin in the histogram, and more than 40% are between $10\,s$ and $115\,s$.

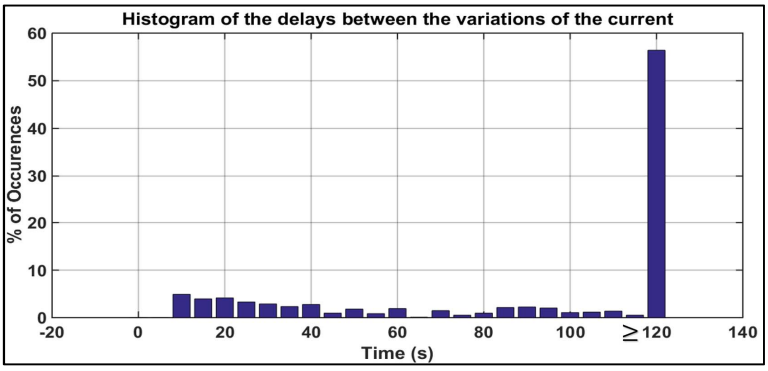

Fig. 5: Histogram of occurrences (in percentage) of the delays between the big variations of the current.

2.2. The resulting accelerated ageing profile

By taking into account the characteristics of the photovoltaic mission profile, this study suggests the accelerated ageing profile presented in Fig. 6.a. This profile simulates one day of real application (without considering the night). Like in the real application, the maximum RMS current profile has a sinusoidal shape (section 2.1.1.) and the minimum current value at a given time is 10% of the current's

value before the occurring of the variation (section 2.1.2.). So the variation of the current at a given time can be expresses as $\Delta I = 0.9 \cdot I_{Clear}$, where I_{Clear} is the RMS current's value before the variation (corresponding to a clear sky). This can be seen in Fig. 6.b. that represents a zoom on Fig. 6.a.

On the other hand it can be noticed that a truncation is applied at the two extremes of the profile, so that the value of the current starts at I_{LIMIT} instead of 0, to prevent the creation of ΔT_J < 30 K (by introducing $\Delta I \geq \Delta I_{min}$). I_{MAX} represents the peak value of the RMS current.

As described in section 2.1.5. , and as it can be seen in Fig. 6.a., the ambient temperature T_a has a sinusoidal shape varying from $T_{a_{min}}$ to $T_{a_{max}}$ In Fig. 6.b. and as described in the section 2.1.3. the slope $\frac{\Delta I}{\Delta t} = 0.15 \cdot I_{MAX}$ (A/s), and T_{on} and T_{off} (section 2.1.6.) represent the delays between the variations.

Finally, since the 4 seasons show the same characteristics, it was chosen to represent them all with a unique profile. This current profile is applied sequentially during the power cycling, using the opposition method, by switching the semiconductors of the inverter using the PWM, and a thermal cycling is applied simultaneously by varying the ambient temperature. A pause $T_p = 15\ minutes$ is made between two consecutive profiles to allow for the relaxation of the viscoelastic constraints in the module [12] [13].

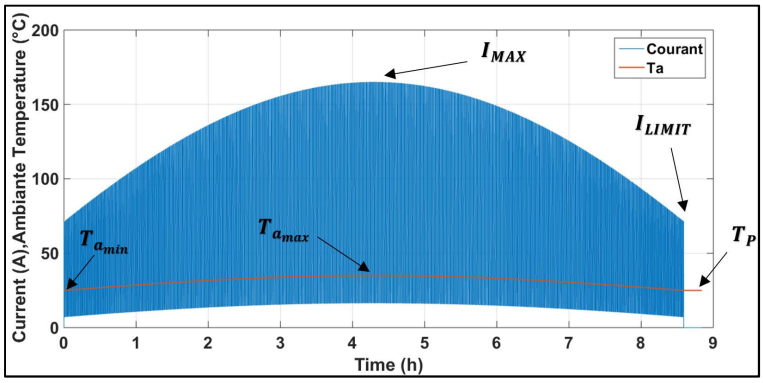

a. Ageing profile simulating one day of real application.

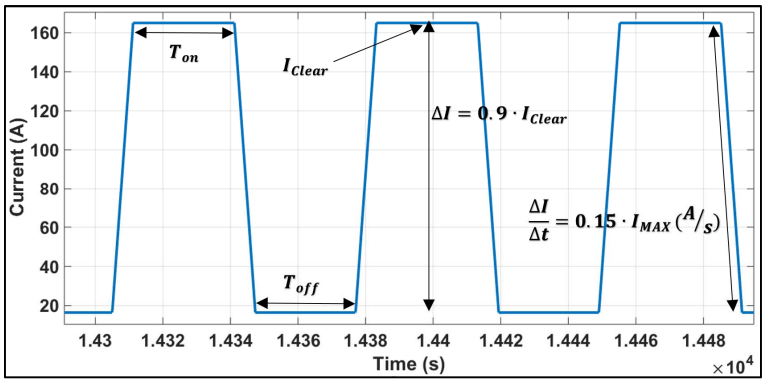

b. Zoom on several current variations.

Fig. 6: The accelerated ageing profile of the current and the ambient temperature.

3. Implementation of the method

3.1. The case study

This method is applied to a photovoltaic 3 phase 2 levels inverter with a DC bus voltage E of 1200 V and a phase to phase output voltage of 690 V, with the grid frequency f_{bf} = 50 Hz, using a modulation factor m = 0.95 and a switching frequency f_C=20 kHz, with a power factor cosφ = 1. SiC MOSFETs modules, with Schottky diodes in antiparallel, are used in the inverter, and have a voltage rating of 1700V and a current rating of 225A, with a maximum junction temperature $T_{J_{max}} = 150\ °$.

Finally the heatsink of the inverter, used in this study was chosen to have a thermal time constant of $\tau_H = 10$ corresponding to a liquid cooler (with a simplified modeling approach).

3.2. Power losses and thermal models

As mentioned in in the Introduction section (Fig. 1), a power losses estimation model is used, followed by a thermal model to estimate, for a given current profile, the corresponding average junction temperature of the power devices T_J . These models are built with Matlab, and use advanced equations to shorten the computation time for mission profiles of several years with an important amount of samples [4]. The electro-thermal coupling is used to take into account the dependence of some electrical parameters of the power loss model to the junction temperature.

The thermal model is based on the use of thermal impedances $Z_{th_{CH}}$ (Case-Heatsink), $Z_{th_{HA}}$ (Heatsink-Ambient) and $Z_{th_{JC}}$ (Junction-Case). The global thermal impedance can be determined according to the Foster model [4] [14]. This thermal impedance represents the image of the step response of the system, which is the temperature response to a constant power step, applied to the electrical equivalent model.

These two models described in details in [15], use the power module thermal impedances given in the datasheet to estimate the junction temperature profile which correspond to the introduced current profile. Considering the heatsink time constant $\tau_H = 10s$ in one hand, and the histogram presented in Fig. 5, in the other hand, where more than 85% of the delays between the variations are higher than $30s$ $(= 3\tau_H)$, and by using these power estimation and thermal models, T_{on} and T_{off} were chosen to be equal to $30s$ to maximize the number and amplitudes of temperature swings ΔT_J. Also by using these models, ΔI_{min} was determined to be equal to 43% of I_{MAX} . It was noticed that the variations of the junction temperature can be maximized for accelerating the ageing process, by variating this temperature between $T_{a_{min}} = 25\ ^\circ C$ and $T_{a_{max}} = 35\ ^\circ C$.

The resulting junction temperature profile is presented in Fig. 7.a. As it can be seen, the maximum junction temperature reaches 130°C and, at the end of the profile, it regains 25°C along $T_p = 15\ min$, before the next repetition of the profile. Fig 7.b. represents a zoom on Fig. 7.a. where each cycle lasts slightly longer than $1\ min$ $(T_{on} + T_{off} +$ rising and falling times.)

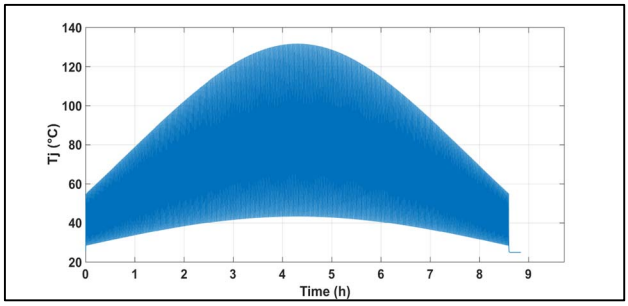

a. Ageing profile representing the junction temperature of a cycle, simulating one day.

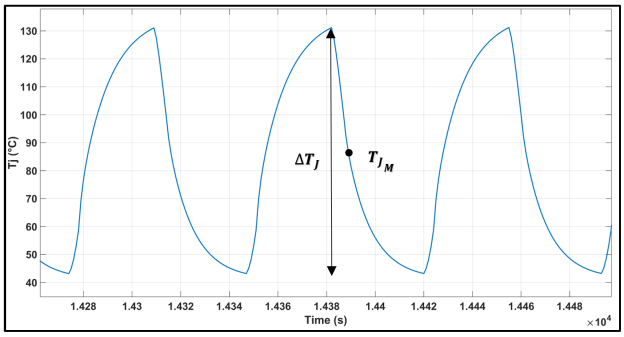

b. Zoom on several junction temperature variations.

Fig. 7: Accelerated ageing profile of the junction temperature over a fundamental period corresponding to $f = 50Hz$.

3.3. "Rainflow Algorithm" and comparison

"Rainflow Algorithm" is a cycle counting algorithm (cycles contained in a mission profile). The junction temperature profile of power MOSFETs in Fig. 7.a. represents the input of this algorithm, which gives as an output the number of occurrences N of each value of ΔT_J at a given level of average T_J (T_{J_M}), represented in form of histograms $N = f(T_{J_M}, \Delta T_J)$ [16] [17]. T_{J_M} represents the average value of a given cycle (Fig. 7.b.). By applying this algorithm on the temperature profiles obtained, comparative histograms of ΔT_J and T_{J_M} for the measured profile and the accelerated ageing profile can be established. These histograms are presented in Fig. 8.a. and Fig. 8.b.

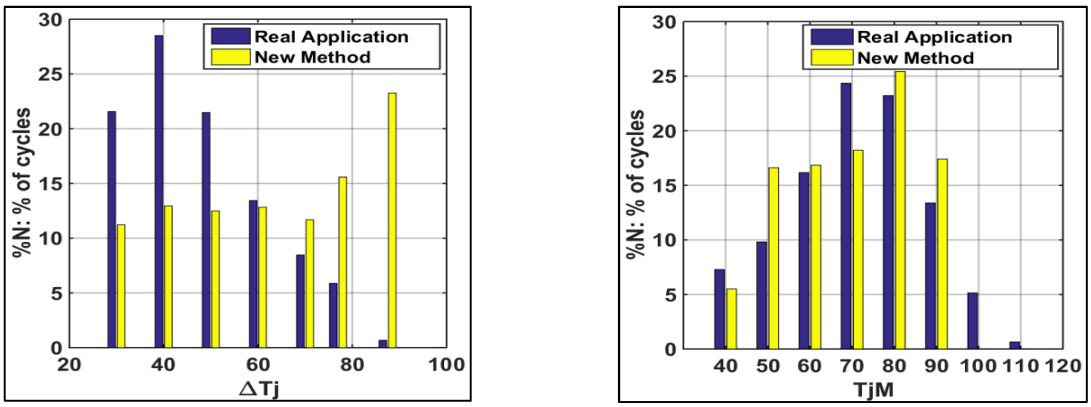

a. $\%Number\ of\ cycles = f(\Delta T_J)$ b. $\%Number\ of\ cycles = f\left(T_{J_M}\right)$

Fig. 8: Histograms of the percentage of the junction temperature cycles number, presented as a function of respectively the temperature variation value, and the average temperature value of the cycles.

In Fig. 8, the number of cycles is presented in percentage because the total number of cycles for the measured profile, over one year, is much higher than the one of the accelerated ageing method (over 8 hours). A fair and easier comparison can then be done on the distribution of ΔT_J (Fig. 8.a.) and T_{J_M} (Fig. 8.b.). It can be noticed on these histograms that the new method represents the application better than the traditional power cycling, which uses just one value for T_{J_M} and ΔT_J.

Although the new method reproduces close values of T_{J_M}, the repartitions of ΔT_J are still not the same. The proposed method reproduces more ΔT_J with high values, and less ΔT_J with low values. Even if it is interesting to increase the number of high ΔT_J to accelerate the ageing of the devices, the next section will propose a method to obtain a refinement of the profile by improving the similarity with the real application.

4. Refinement of the accelerated ageing profile

To reduce the dissimilarities in the histograms of ΔT_J and T_{J_M} presented in Fig. 8, a refinement of the accelerated ageing profile of section 2.2. should be done. In this sense, all the variations of the RMS current which exist in the real measured profile, and which generate $\Delta T_J \geq 30$K were integrated in the new refined profile. So instead of introducing the variations of the current $\Delta I = 0.9 \cdot I_{Clear}$ (as in the case of the first profile), which is the maximum value of the variations caused by the passage of clouds, the new profile reproduces the real ΔI of the measured current with small modifications.

It should be noticed that the two accelerated ageing profiles have the same values of $\frac{\Delta I}{\Delta t}, T_{on}, T_{off}, I_{LIMIT}, T_P$, and the only differences remain in ΔI and T_a. The ambient temperature T_a, still have a sinusoidal evolution, but the values of $T_{a_{min}}$ and $T_{a_{max}}$ are modified.

After introducing the new accelerated ageing profile into the thermal model, the "Rainflow Algorithm" is applied to the junction temperature profile. After several refinements made by applying small modifications in the values of the ambient temperature and the real ΔI, the refined accelerated

ageing profile was obtained and is presented in Fig. 9.a. with a zoom on it in Fig. 9.b., with an ambient temperature varying between 25 °C and 40 °C.

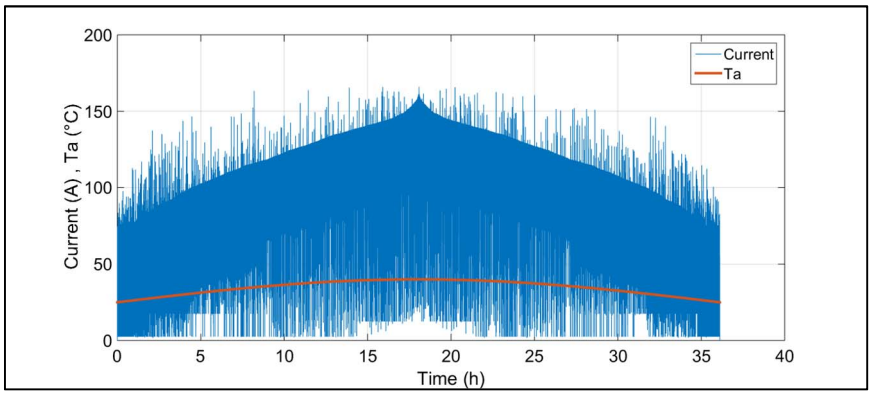

a. The refined ageing profile, accumulating all the big variations that occurred during one year.

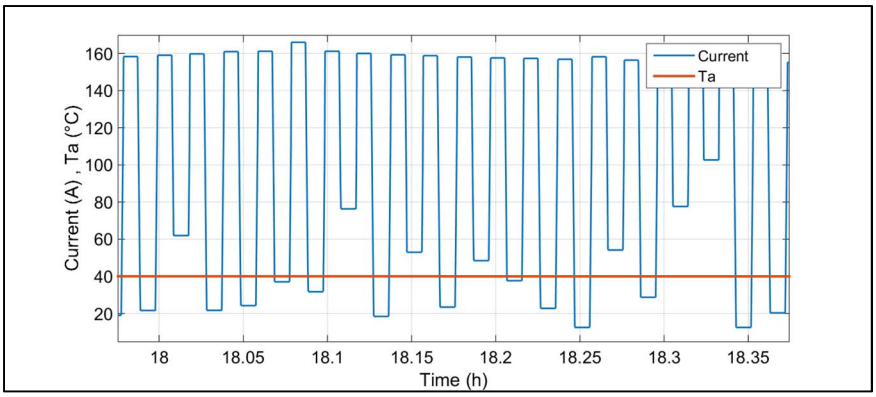

b. Zoom on several current variations.

Fig. 9: The refined accelerated ageing profile of the current and the ambient temperature.

The two comparative histograms obtained with the "Rainflow Algorithm" are presented in Fig. 10. These histograms compare the percentage of the junction temperature cycles number presented as a function of, respectively, the temperature variation value and the average temperature value of cycle, between the accelerated ageing profile obtained with the new method, the measured profile, and an example of profile obtained using the traditional power cycling method with constant T_{J_M} and ΔT_J, using $T_{on} = 15s - T_{off} = 15s$. As it can be noticed in Fig. 10, with the refined accelerated ageing profile, similar ΔT_J and T_{J_M} of the real application were reproduced.

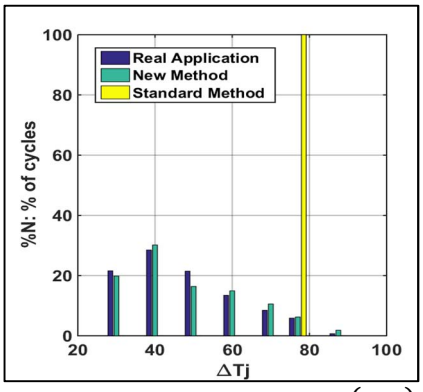

a. $\%Number\ of\ cycles = f(\Delta T_J)$

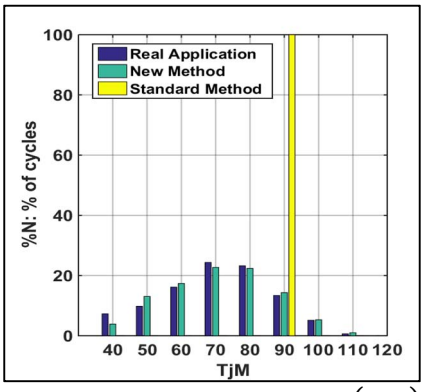

b. $\%Number\ of\ cycles = f\left(T_{J_M}\right)$

Fig. 10 Histograms of the percentage of the junction temperature cycles number, presented as a function of respectively the temperature variation value, and the average temperature value of the cycles.

5. Results and lifetime estimation

Having no specific lifetime estimation model for the power module used in this study, and aiming to compare the tests time of the classical power cycling with the new method, a lifetime estimation model from the literature was used. In fact, the literature presents multiple models [18] [19], and a model presented in [4] [20] was chosen to do the comparison, because it takes into consideration a lot of parameters like the blocking voltage rating of the chip (V_C), diameter (D) of the bonding wire, current per wire (I_B) and the pulse duration (t_{on}). Table I represents the results of the accelerated ageing tests after applying this model. For the classical power cycling as presented in Fig. 10, $T_{J_M} = 90°C,\ \Delta T_J = 80K, T_{on} = T_{off} = 15s$.

Table I Comparison of different tests durations.

	Real application	Classical Power cycling	New method (1st profile)	New refined method (2nd profile)
Test time (Days)	4320 (~12 years)	40.9 (~1.5 months)	73 (~2.5 months)	153.5 (~5 months)

It can be noted from Table. 1 that the classical power cycling is the fastest among the presented ageing tests and that the method using the second profile is the slowest, but it is also the one that better represents the photovoltaic application. The method using the first profile is a compromise between the speed and the representation of the application. It should be noted that the values presented in this table are used only to compare the different methods, and should not be considered representative as the power module used in this study does not have a lifetime estimation model.

6. Conclusion

This paper presents a new method for the accelerated ageing of photovoltaic inverters, created by analyzing the mission profiles of the current and ambient temperature, extracted over several years from multiple photovoltaic plants.

This method combines power cycling using the opposition method with thermal cycling, and suggests two accelerated ageing mission profiles. Although being slower than the classical power cycling test, this method is expected to provide more representative results, and thus reducing the favoring of certain failure modes to the detriment of others.

This method can be used to reveal the weak points of the power modules used in photovoltaic inverters, thus proposing more robust power module designs dedicated to photovoltaic applications.

References

[1] C. Sintamarean, H. Wang, F. Blaabjerg, F. Iannuzzo, "The Impact of Gate-Driver Parameters Variation and Device Degradation in the PV-Inverter Lifetime", Proceedings of the IEEE Energy Conversion Congress and Exposition (ECCE 2014), Pittsburgh, PA, USA,14-18 September, 2014.

[2] J. M. Thebaud, E. Woirgard, C. Zardini, S. Azzopardi, O. Briat and J. M. Vinassa, "Strategy for designing accelerated aging tests to evaluate IGBT power modules lifetime in real operation mode", in IEEE Transactions on Components and Packaging Technologies, vol. 26, no. 2, pp. 429-438, June 2003. doi: 10.1109/TCAPT.2003.815112

[3] ECPE Tutorial, "Thermal Engineering of Power Electronic Systems Part II", Oct 18th-19th., 2016, Nuremberg, Deutschland.

[4] A. Wintrich, U. Nicolai, W. Tursky, T. Reimann, “Application Manual Power Semiconductors”, ISLE Verlag 2011.

[5] V. Smet et al., "Ageing and Failure Modes of IGBT Modules in High-Temperature Power Cycling," in IEEE Transactions on Industrial Electronics, vol. 58, no. 10, pp. 4931-4941, Oct. 2011. doi: 10.1109/TIE.2011.2114313

[6] U. M. Choi; F. Blaabjerg; S. Jorgensen, "Power Cycling Test Methods for Reliability Assessment of Power Device Modules in respect to Temperature Stress," in IEEE Transactions on Power Electronics , vol.PP, no.99, pp.1-1. doi: 10.1109/TPEL.2017.2690500

[7] Bahman, A.S., Iannuzzo, F., Blaabjerg, F. "Mission-profile-based stress analysis of bond-wires in SiC power modules", Microelectronics Reliability, Volume 64, September 2016, pp. 419-424, 2016.

[8] R. Schmidt, F. Zeyss, and U. Scheuermann, “Impact of absolute junction temperature on power cycling lifetime,” in Proc. of 15th European Conf. on Power Electronics and Applications (EPE), 2013, pp. 1–10.

[9] Y. Wang, S. Jones, A. Dai, G. Liu, "Reliability enhancement by integrated liquid cooling in power IGBT modules for hybrid and electric vehicles", Microelectronics Reliability, vol. 54, no. 9–10, pp. 1911-1915, Sep./Oct. 2014.

[10] E. Matagne, R. El Bachtiri, "Exact analytical expression of the hemispherical irradiance on a sloped plane from the Perez sky", Solar Energy, Volume 99, January 2014, Pages 267-271, doi:10.1016/j.solener.2013.11.016

[11] Rakovec J, Zak sek K, "On the proper analytical expression for the sky-view factor and the diffuse irradiation of a slope for an isotropic sky", Renewable Energy), Volume 37, Issue 1, January 2012, Pages 440-444, doi:10.1016/j.renene.2011.06.042

[12] G. Grossmann, G. Nicoletti and U. Soler, "Results of comparative reliability tests on lead-free solder alloys," 52nd Electronic Components and Technology Conference 2002. (Cat. No.02CH37345), 2002, pp. 1232-1237.doi: 10.1109/ECTC.2002.1008264

[13] M. Ciappa, F. Carbognani and W. Fichtner, "Lifetime prediction and design of reliability tests for high-power devices in automotive applications," in IEEE Transactions on Device and Materials Reliability, vol. 3, no. 4, pp. 191-196, Dec. 2003.doi: 10.1109/TDMR.2003.818148

[14] J. Lutz, H, Schlangenotto, U. Scheuermann, R.De Doncker, "Semiconductor Power Devices: Physics, Characteristics, Reliability", Springer-Verlag Berlin Heidelberg, ISBN 978-3-642-11125-9, 2011.

[15] M.Dbeiss, Y.Avenas, H. Zara., "Estimation des contraintes électrothermiques sur les composants semi-conducteurs dans les onduleurs photovoltaïques", Proceedings of SGE conference, Grenoble, France, 2016.

[16] A. Niesłony, "Determination of fragments of multiaxial service loading strongly influencing the fatigue of machine components", Mech. Syst. Signal Process., vol. 23, no. 8, pp. 2712-2721, 2009.

[17] K. Mainka, M. Thoben and O. Schilling, "Lifetime calculation for power modules, application and theory of models and counting methods", Proceedings of the 2011 14th European Conference on Power Electronics and Applications, Birmingham, 2011, pp. 1-8.

[18] M. Held, P. Jacob, G. Nicoletti, P. Scacco and M. H. Poech, "Fast power cycling test of IGBT modules in traction application", Proceedings of Second International Conference on Power Electronics and Drive Systems, 1997, pp. 425-430 vol.1.doi: 10.1109/PEDS.1997.618742.

[19] U. Scheuermann and R. Schmidt, “A new lifetime model for advanced power modules with sintered chips and optimized Al wire bonds”, in Proc. of Int. Exhibition and Conf. for Power Electronics, Intelligent Motion, Renewable Energy and Energy Management (PCIM), Nuremberg, Germany, 2013, pp. 810–817.

[20] R. Bayerer, T. Herrmann, T. Licht, J. Lutz and M. Feller, "Model for Power Cycling lifetime of IGBT Modules - various factors influencing lifetime",5th International Conference on Integrated Power Electronics Systems, Nuremberg, Germany, 2008, pp. 1-6.